Carbohydrate Polymers 100 (2014) 40–45

Contents lists available at ScienceDirect

Carbohydrate Polymers

journal homepage: www.elsevier.com/locate/carbpol

A cellulosic responsive "living" membrane

Guokui Qin, Bruce J. Panilaitis*, Zhongyuan Sun David L. Kaplan

Department of Biomedical Engineering, 4 Colby Street, Tufts University, Medford, MA 02155, USA

ARTICLE INFO

Article history:
Received 8 January 2013
Received in revised form 9 May 2013
Accepted 14 June 2013
Available online 28 June 2013

Keywords:
Living membrane
Bacterial cellulose
Co-cultivation
Gene amplifier
Positive feedback

ABSTRACT

Bacterial cellulose has been demonstrated to be a remarkably versatile biomaterial and widely used in biomedical applications due to its unique physical properties. Here we reported for the first time a "living membrane" system based on recombinant *Escherichia coli* bacterial strains entrapped in cellulosic membranes produced by *Gluconacetobacter xylinus*. Biologically driven detection and identification of a range of target molecules presents unique challenges, and requires that detection methods are developed to be rapid, specific and sensitive. The compatibility of *G. xylinus* and recombinant *E. coli* strains was first investigated for co-cultivation, and the relationship between the number of entrapped *E. coli* and the level of inducible signal achieved was further explored by fluorescent signal observation in confocal microscopy. Finally to amplify the response to inducers for maximum fluorescent signal, a positive-feedback genetic amplifier was designed within recombinant *E. coli* strain entrapped in the living cellulosic membrane system, allowing for the detection mechanism to be extremely sensitive and resulting in a significant fluorescent signal from a single receptor binding event. The living membrane system proposed here will create devices of greater complexity in function for applications in biological and chemical detection.

1. Introduction

Bacterial cellulose has been widely reported in several applications due to its unique physical properties such as higher mechanical strength, water absorption capacity and higher crystallinity, as well as an ultra-fine and highly pure fiber network structure (Charreau, Foresti, & Vazquez, 2012; Thomas, 2008; Yadav, Paniliatis, Shi, Lee, Cebe, & Kaplan, 2010). It has been demonstrated to be a remarkably versatile biomaterial and considered for biomedical applications including wound healing, tissue regeneration, and drug delivery and release (Mayer et al., 1991; Nagai, Nishibe, Makino, Tomimori, & Yamada, 1997; Thomas, 2008). *Gluconacetobacter xylinus* is the most efficient bacterial cellulose producer and has been used as the model system for cellulose biosynthesis (Aloni, Delmer, & Benziman, 1982; Lin, Brown, Cooper, & Delmer, 1985). Typically an extracellular cellulose produced is deposited as a continuous pellicle (membrane) at the gas–liquid interface of a static culture that entraps the bacteria itself and any co-cultured organisms as it grows (Gretz, Folsom, & Brown, 1989). The pellicle is permeable to small protein molecules and its thickness is directly proportional to the duration of cultivation, providing a natural filter for processing of test samples and excellent mechanical properties when compared to cellulose of plant origin. A great number of studies have been completed on the production, physical structure and the chemical composition of bacterial cellulose (Kim, Lee, & Torget, 2001; Lee et al., 2001; Ross et al., 1987; Son, Heo, Kim, & Lee, 2001). For example, the cellulose exhibited strong antiviral activity *in vitro* after chemical modification by sulfation with piperidine *N*-sulfonic acid (Kojima et al., 1991). Several studies have been reported to generate chimerical cellulosic copolymers with non-glucose monomers or containing other polymers, including chitin and chitosan (Kim et al., 2001; Plumbridge, 1995; Yadav et al., 2010). Our most recent work has successfully incorporated heterologous genes into *G. xylinus* with a metabolic engineering-based approach to the rational redesign of cellular metabolites, allowing incorporation of *N*-acetyl-glucosamine (GlcNAc) at much higher levels than previously observed (Yadav et al., 2010; Yadav, Panilaitis, Shi, Numuta, Lee, & Kaplan, 2011). The resulting cellulose-chitin copolymer was demonstrated to be *in vivo* degradable, providing a new route to overcome the longstanding limitation associated with the poor degradability of cellulose for biomedical and biomass conversion applications.

Current detection of target molecules including pathogen and chemical detection often utilizes sophisticated equipment that is fragile and requires significant power supply, and dedicated laboratory space that is not available in all locations (Chepurnykh & Avkhimenko, 1994; Ligon, 2006; Upadhyayula, 2012). A rapid, simple, and low cost detection technology with high sensitivity is needed for stability and functionality at extremes of temperature, humidity and in the absence of elaborate support equipment. Bacteria naturally respond to a wide range of stimuli in their environment. Most of those systems are designed to respond to

* Corresponding author. Tel.: +1 617 627 3607; fax: +1 617 627 3231.
E-mail address: bruce.panilaitis@tufts.edu (B.J. Panilaitis).

0144-8617/$ – see front matter © 2013 Published by Elsevier Ltd.
http://dx.doi.org/10.1016/j.carbpol.2013.06.019

Table 1
Bacterial strains and plasmids used in this study.

Strains or plasmids	Relevant features or description	Source and purpose
Strains		
G. xylinus ATCC 10245	Wild type (wt); standard cellulose production	ATCC; this study
E. coli NEB5α	Gene cloning	NEB; cloning
E. coli BLR (DE3)	High protein expression	Novagen; expression
E. coli BL21star (DE3)	High protein expression	Invitrogen; expression
Plasmids		
pGFPuv	Amp^r; green fluorescent protein (GFP) gene	Clontech; GFP expression
pJexpress-RFP	Kan^r; red fluorescent protein (RFP) gene	DNA2.0; RFP expression
pGEM-T	Amp^r; PCR cloning vector	Promega; cloning
pGEMT-GFP/Lux	Amp^r; recombinant plasmid harboring GFP/lux gene	This study
pGN68	Cam^r; recombinant plasmid harboring GFP/lux gene with *lux* promoter	Nistala et al. (2010)

Amp^r, ampicillin resistance; Kan^r, kanamycin resistance; Cam^r, chloramphenicol resistance.

small molecules related to nutrient concentration, quorum sensing, or related functions (Dark, Dean, & Warhurst, 2009). For example, Nistala et al. constructed a modular genetic amplifier in *Escherichia coli* for a one-component tetracycline sensor and a two-component aspartate sensor with the increased sensitivity, based on a constitutively active, autoinducer-independent variant of the quorum-sensing regulator LuxR from *Vibrio fischeri* (Nistala, Wu, Rao, & Bhalerao, 2010).

Given the need to respond to larger molecules in the case of some detection applications, here we developed a "living membrane" system based on recombinant bacterial strains entrapped in cellulosic membranes, making them resistant to environmental degradation and persistent for short or long periods of time. Based on the reporter genes available, we have coupled the natural detection capabilities in bacteria with the expression of specific fluorescent proteins to eventually generate a suite of living detectors for the rapid and specific identification of relevant target molecules. Herein we attempt to engineer a genetic amplifier in *E. coli* to amplify a transcriptional fluorescence signal output entrapped in cellulosic membranes, based on the quorum-sensing regulator LuxR as reported previously (Nistala et al., 2010). The proposed system will be durable and easy to use, requiring no additional power or sophisticated support equipment.

2. Materials and methods

2.1. Bacterial strains, culture media and growth conditions

All bacterial strains and plasmids used in this study are listed in Table 1. The cellulose producing bacterium *G. xylinus* strain 10245 was obtained from ATCC (Manassas, VA) and cultured in Hestrin and Schramm (HS) medium (0.5% yeast extract, 0.5% peptone, 0.27% Na_2HPO_4, 0.15% citric acid, pH 4.5) supplemented with 2% glucose and grown at 30 °C shaking at 200 rpm or statically. All of *E. coli* cells were cultured in Luria-Bertani (LB) broth at 37 °C unless noted otherwise. Antibiotics were used at the following concentrations: ampicillin at 100 μg/ml, chloramphenicol at 20 μg/mlm and kanamycin at 50 μg/ml. Primers were purchased from Invitrogen Inc. (Carlsbad, CA). Restriction enzymes were purchased from New England Biolabs Inc. (Ipswitch, MA) and used according to the manufacturer's recommendations. All cloning steps were performed in *E. coli* strain NEB5α (New England Biolabs, Ipswitch, MA). Subsequent experiments involving the protein expression under IPTG induction were conducted in *E. coli* strain BL21 star (DE3) (Invitrogen, Carlsbad, CA) and strain BLR (DE3) (Novagen, Madison, WI).

2.2. Plasmid construction and transformation

The plasmid pGN68 with the chloramphenicol selection gene (Nistala et al., 2010) (donated by Prof. Kaustubh Bhalerao, University of Illinois at Urbana-Champaign, USA) was made for the *luxI-GFP-LuxR* transcriptional fusion with the *luxI* promoter. The GFP–LuxR fusion of the GFP and LuxR genes was first PCR amplified using the plasmid pGN68 as the template with the primers GN10F (GGG GAA TTC ATA CGT ATT TAA ATC AGG AGT GGA AAT GAG TAA AGG AGA AGA ACT T) and KW171R (AAT AGC GGC CGC TTA TTA ATT TTT AAA GTA TGG GC) (Nistala et al., 2010). The PCR program was used as follows: 95 °C for 4 min (1 cycle); 95 °C for 30 s, 60 °C for 30 s, 72 °C for 1.5 min (30 cycles) and 72 °C for 10 min (1 cycle). The resulting amplified DNA fragments of approximately 1 kb were gel extracted (Qiagen, Valencia, CA) and then cloned into the *BamH*I and *Not*I restriction sites of the vector pGEM-T (Promega, Madison, WI), yielding the new plasmid pGEMT-GFP/LuxR with the *T7* promoter. Ligation reactions were done using T4 DNA ligase (Invitrogen, Carlsbad, CA) at 16 °C. The ligation product was used to transform *E. coli* DH5α strain (Invitrogen, Carlsbad CA) and successful transformants were identified by plating and incubation on a LB/agar plate containing 100 μg/ml ampicillin. The presence of correct inserts in each construct was identified by colony PCR and confirmed by DNA sequencing.

The plasmid pGFPuv (Clontech, Mountain View, CA) with the ampicillin selection gene was transformed into *E. coli* BLR (DE3) for the expression of green fluorescent protein (GFP). The plasmid pJexpress-RFP (DNA2.0, Menlo Park, CA) with the kanamycin selection gene was transformed into *E. coli* strain BL21 star (DE3) for the expression of red fluorescent protein (RFP). The new plasmid pGEMT-GFP/Lux with the ampicillin selection gene was also transformed into *E. coli* BL21 star (DE3) for GFP expression. A genetic amplifier with the plasmid pGN68 and plasmid pGEMT-GFP/Lux was further transformed into the same *E. coli* BL21 star (DE3) for GFP signal detection.

2.3. Cell growth, cellulose production, and fluorescent protein expression

For cellulose production in static culture, *G. xylinus* strain 10245 cells were grown in 6-well culture plates containing 10 ml of HS medium each well at 30 °C for 1 week. The cellulose pellicles were purified by treating twice with 4% SDS solution at 70 °C for 4 h and 4% NaOH at 70 °C for 4 h to remove the entrapped bacteria, followed by several washes with deionized water as reported previously (Yadav et al., 2010). The purified cellulose mats were further dried at 70 °C for 30 h for next studies. To develop a "living" membrane system with fluorescent signals, *G. xylinus* strain 10245 cells were grown in 6-well culture plates at the same conditions for 4 days, and 2% (v/v) *E. coli* cells harboring the plasmids were then applied into each well and co-cultured with *G. xylinus* cells at 30 °C for 8–12 h. Finally fluorescent protein expression was induced by adding 1 mM ITPG (isopropyl β-D-thiogalactoside) (Fisher Scientific, Hampton, NH) into each well of plates and measured after

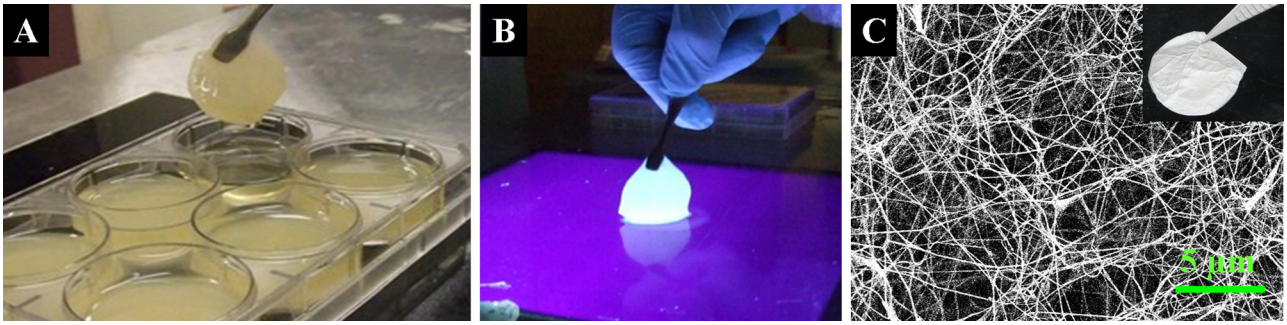

Fig. 1. Cellulose production and morphology. (A) The cellulose membrane (pellicle) produced by *G. xylinus* strain 10245; (B) GFP fluorescent signal expressed within *E. coli* BLR (DE3) entrapped in the cellulose membrane observed under UV light; and (C) the morphologies of freeze-dried cellulose pellicles studied by SEM.

further incubation at 30 °C for 8–12 h (Qin et al., 2009, 2011). Following the same steps, different cell numbers of *E. coli* were loaded into different well of the same plate to examine the relationship between the number of entrapped *E. coli* and the level of inducible signal achieved.

2.4. Confocal microscopy

The resulting cellulose pellicles generated with *G. xylinus* strain 10245 with entrapped *E. coli* cells were washed twice in sterilized PBS, and then washed several times with deionized water.

The fluorescent signal from each individual cellulose pellicle was assessed using confocal microscopy. Images were obtained using a confocal laser scanning microscope (Leica SP2 inverted microscope) equipped with argon (488 nm) and HeNe (534 nm) lasers. The region of interest was selected from *z* plane images to include either the surface or the internal fibers, beginning with a bottom section at least 1 mm above the surface of the pellicles. Depth projection micrographs were obtained from 20 horizontal sections imaged at a depth distance of 10–20 mm from each other. The fluorescent signal intensity and three-dimensional multichannel-image processing was determined and analyzed by using ImageJ (Mandal, Grinberg, Gil, Panilaitis, & Kaplan, 2012; Park et al., 2012).

2.5. Scanning electron microscopy (SEM)

SEM was used to assess additional morphological characterization of the freeze-dried cellulose pellicle samples (Yadav et al., 2010). The experiments were performed using a Zeiss 55VP System (Oberkochen, Germany, at Harvard University Center for Nanoscale Systems, Cambridge, MA). Freeze-dried samples were first mounted on a silicon chip in a closed container at room temperature. SEM images were collected, after sputter coating (Cressington, 208HR) with a Pt/Pd target, using both InLens and secondary backscatter detectors.

3. Results and discussion

3.1. Cellulose production and morphology

To produce bacterial cellulose production, *G. xylinus* strain 10245 was grown in static culture at 30 °C for up to 7 days. The resulting cellulose was deposited as an extracellular pellicle which was extracted from the HS medium. Typically the cellulose polymer accumulates at the gas–liquid interface of a static culture as a continuous membrane (pellicle) as shown in Fig. 1A. The pellicle thickness is directly proportional to the duration of cultivation, generally limited by media carbon source and pH. In the studies presented here, the pellicles were approximately 5 mm thick. The cellulose pellicle could be further treated and purified into different forms based on different studies. For example, the pellicles can be dried into a cellulose film or freeze-dried into a cellulose mat after purification. The cellulose membrane has an ability to entrap the cellulose-producing bacteria themselves together with other bacteria within the same membrane system. As an example reported here, *E. coli* cells with green fluorescent protein (GFP) expressed under IPTG induction were inoculated into the cellulose membrane, and then fluorescence signal under UV light was observed from the cellulose membrane, indicating the ability of entrapment for the cellulose membrane produced by *G. xylinus* strain 10245 (Fig. 1B). Freeze-dried cellulose pellicle morphology was assessed by SEM, showing the arrangement of associated thin fibers (Fig. 1C).

3.2. Co-culture capability and fluorescent signal measurement

The preliminary data obtained above validated the *in situ* generation of cellulosic membranes that encapsulate secondary catalytic organisms. To examine the compatibility of the cellulose producing organism *G. xylinus* and recombinant *E. coli* strains to co-cultivation in terms of gross viability, we attempted co-cultivation first through the seeding of membrane surfaces with *E. coli* BLR (DE3) harvested during log phase from a primary culture. After the cellulose membranes were produced by *G. xylinus* in HS medium for 4 days, the secondary organism *E. coli* cells were inoculated and grown in the same HS medium for three days, allowing for the differential quantification of cellulose productivity and cell viability of both organisms. In order to assist in cell counts, we transformed the plasmid pGFPuv into *E. coli* BLR (DE3) and plasmid pJexpress-RFP into *E. coli* BL21 star (DE3) for GFP and RFP signal expression respectively, and then we determined secondary bacterial density and location in intact membranes by confocal microscopy. The GFP and RFP signal expressed by *E. coli* were detected in the cellulose membranes with and without IPTG induction as shown in Fig. 2. Strong fluorescence signal was observed from the combined system with IPTG induction, demonstrating the compatibility of co-cultivation of *E. coli* on *G. xylinus* supportive media.

The fundamental concept of co-cultivation with these novel living membranes may lead to an expanded range of membrane functions. Further efforts can address the growth kinetics and viability of both organisms under a variety of environmental conditions and elucidate the three dimensional structure and composition of resulting polymeric/cellular material. For example, cultivation time is the main determinant of cellulose production and molecular weight (Ross, Mayer, & Benziman, 1991), and membranes produced here grow to thicknesses effective for separations within 24–72 h. Dissolved oxygen (DO) concentrations can affect significantly cellulose production (Setyawati, Chien, & Lee, 2007). The facultative nature of most *E. coli* strains and the relatively low critical oxygen concentrations of *G. xylinus* strains should result in

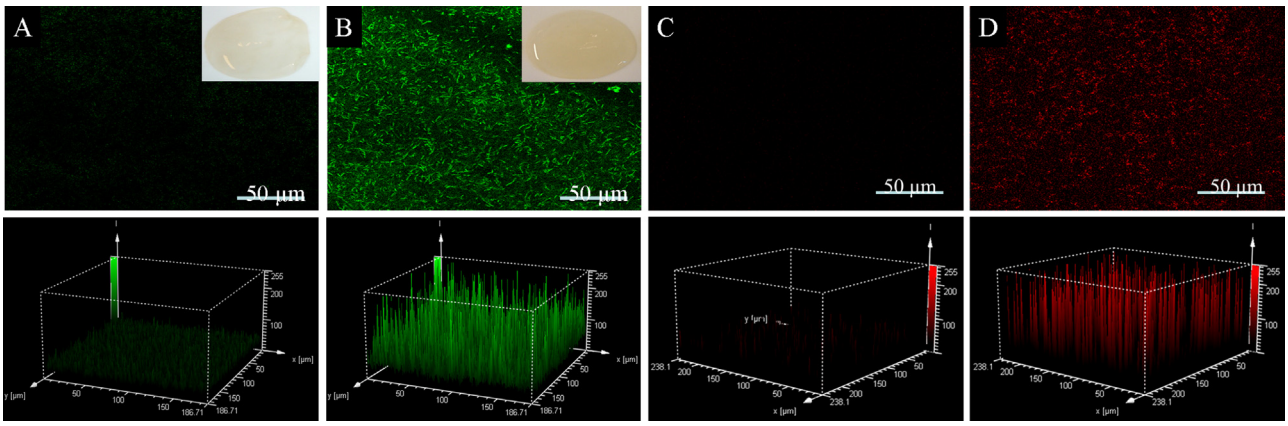

Fig. 2. Co-culture capability and fluorescent signal with 2D (upper) and 3D (lower) measurement. GFP signal expressed within *E. coli* BLR (DE3) was observed in the cellulose membrane without (A) and with (B) IPTG induction. The insert is the cellulose membrane with recombinant *E. coli* entrapped without (A) and with (B) IPTG induction. RFP signal expressed within *E. coli* BL21 star (DE3) was also observed in the cellulose membrane without (C) and with (D) IPTG induction.

the flexibility to maintain baseline populations of each organism under conditions favorable to each other (Chao, Ishida, Sugano, & Shoda, 2000; Henderson & Chenoweth, 1985; Hwang, Yang, Hwang, Pyun, & Kim, 1999). This behavior could be investigated using static cultivation of a continuous cellulose pellicle along a gas/media interface for 4–6 days, followed by shorter agitated cultivation of *E. coli* strains with and without sparging (air). Additional encapsulating cellulosic material could then be cultivated *via* the reduction of oxygenation to static levels, with subsequent entrainment of secondary organisms. Other environmental factors have also been reported to influence the level of cellulose production, such as carbon source, pH and agitation (Kim et al., 2001; Lee et al., 2001; Ryu, Lee, Kim, Kang, & Kim, 2001; Son et al., 2001). Each of these variables could be manipulated in order to find optimal conditions for living membrane development. Here we used GFP or RFP for the signal output as they can provide a facile measure of transcriptional activity, and any other genes can in practice be used as the readout (Nistala et al., 2010).

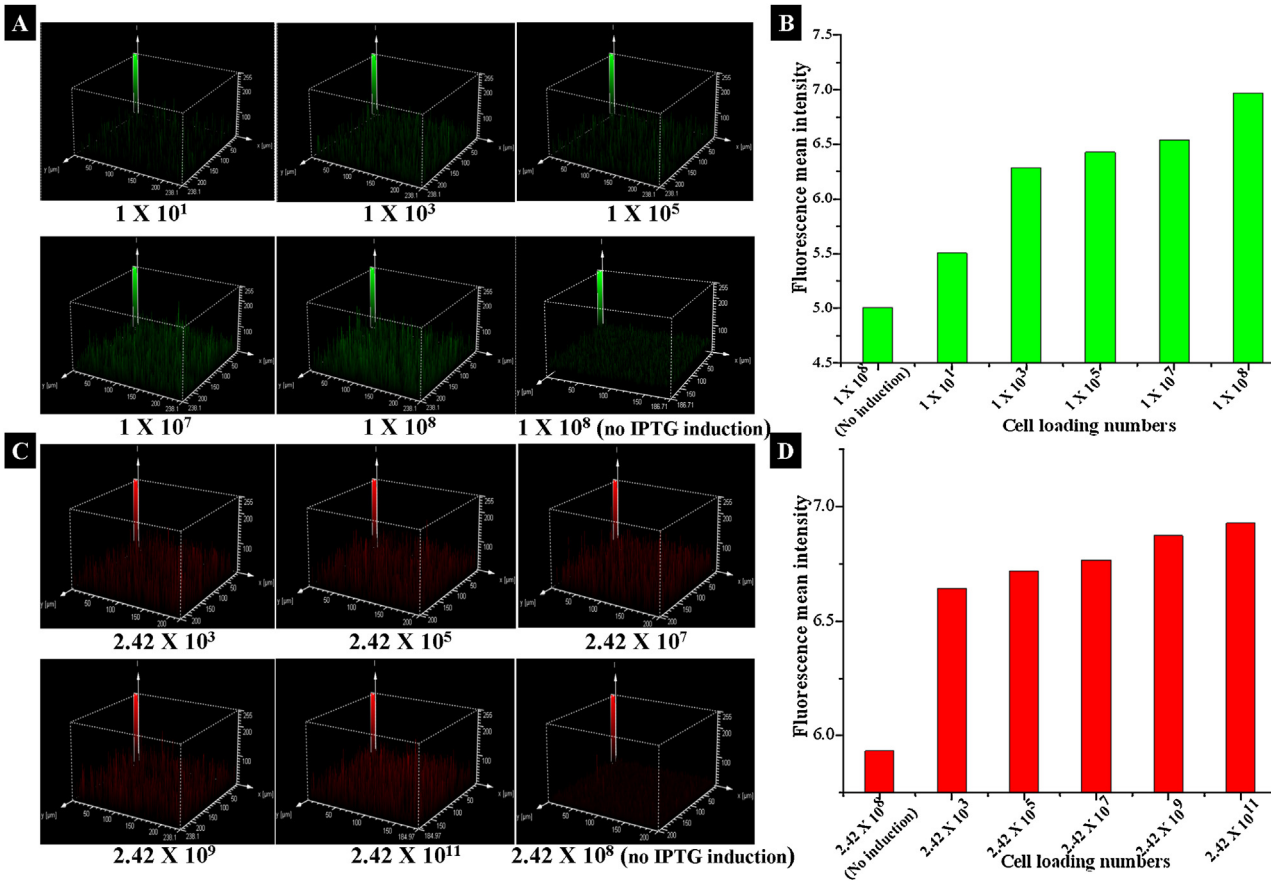

Fig. 3. Bacterial loading capacity and fluorescent signal level. The GFP (A) and RFP (C) fluorescent signals with different loading numbers of *E. coli* cells were observed by confocal microscopy, compared with the signal expression without IPTG induction. The GFP (B) and RFP (D) fluorescent intensity was further analyzed by ImageJ software for comparison of fluorescent signal expression with different loading numbers of *E. coli* cells.

3.3. Bacterial loading capacity and fluorescent signal level

In order to maximize the production of fluorescence signal or cell density within the membranes, the optimum level of entrapped *E. coli* needed to be determined. For this part of the work, we examined the relationship between the number of entrapped *E. coli* and the level of inducible signal which could be achieved. We first selected the *E. coli* strains transformed with the fluorescent marker, GFP or RFP, and then induced a detectable level of GFP or RFP expression by IPTG in control experiments to determine the range of stimuli. After cellulose membranes were produced by *G. xylinus* for 4 days as reported above, different numbers of *E. coli* cells with the fluorescent marker were inoculated and induced by IPTG at the same time for fluorescent signal expression. For detection of GFP expression level, we tried 5 different loading numbers of *E. coli* cells, 1×10^1, 1×10^3, 1×10^5, 1×10^7 and 1×10^8 CFU. The GFP fluorescent signal was observed by confocal microscopy and increased obviously as the *E. coli* cell loading number increased, compared with the signal expression without IPTG induction (Fig. 3A). The GFP fluorescent intensity was further analyzed by ImageJ software for comparison of fluorescent signal expression with different loading numbers of *E. coli* cells. As shown in Fig. 3B, the fluorescent intensity increased obviously from 1×10^1 to 1×10^3 CFU of *E. coli* cell numbers loaded, and showed an apparent dose-dependent increase from 1×10^3 to 1×10^8 CFU of *E. coli* cell numbers loaded. Following the similar strategy, we loaded 5 different quantities of *E. coli* cells for detection of RFP expression level, 2.42×10^3, 2.42×10^5, 2.42×10^7, 2.42×10^9 and 2.42×10^{11} CFU. Both RFP fluorescent signal and intensity were observed by confocal microscopy and analyzed by ImageJ software (Fig. 3C and D), indicating the RFP expression by *E. coli* in the cellulose membranes was increased as the cell loading number increased similar to what was observed in the GFP cells. Based on the data obtained above, we concluded that the higher number of entrapped *E. coli* can achieve the higher level of inducible signal in the cellulose membranes. The minimum loading number of *E. coli* cells was 1×10^3 and 2.42×10^3 CFU for a detectable level of GFP and RFP expression, respectively.

3.4. Design of positive-feedback genetic amplifier

To amplify the response to inducers for maximum fluorescent signal, attempts begin to generate a reporter system that is directly linked to the LuxR system derived from *V. fischeri* within *E. coli* as the LuxR protein is constitutively active and not dependent on the addition of an exogenous inducer (Nistala et al., 2010). Recent work demonstrated a modular positive feedback-based gene amplifier to enhance reporter gene signals using the GFP as the transcriptional readout (Nistala et al., 2010). Using this system, the GFP reporter system was designed such that an induction of IPTG signal will induce expression of the GFP reporter under specific control of the *T7* promoter, as well as the LuxR amplifier signal, which then will induce secondary expression of the GFP and LuxR gene (Fig. 4).

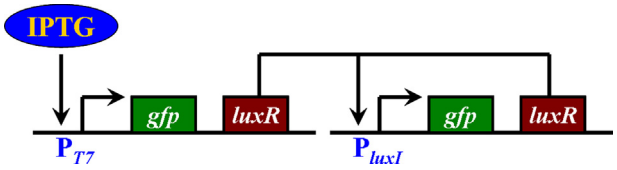

Fig. 4. Schematic of positive-feedback genetic amplifier. The amplifier consists of a plasmid pGN68 where LuxR has been cloned behind the P_{luxI} promoter. The inducer IPTG will bind to the *T7* promoter and control the expression of GFP–LuxR fusion as an output signal. The LuxR produced here was again used to bind to the P_{luxI} promoter, this time as the input signal, and activate secondary expression of GFP–LuxR fusion, which in turn feeds back into the amplifier loop.

In the original plasmid pGN68, the GFP and LuxR genes were arranged behind the P_{luxI} promoter on high-copy number plasmid (ColE1 origin of replication). In this system, LuxR can bind to the P_{luxI} promoter and activate its own transcription. To construct the positive-feedback genetic amplifier we cloned GFP and LuxR genes from plasmid pGN68 behind the *T7* promoter into plasmid pGEM-T, yielding a new plasmid pGEMT-GFP/LuxR (see Section 2 for details). The pGN68 and pGEMT-GFP/LuxR plasmids were transformed together into the *E. coli* strain BL21 star (DE3). In this design, the inducer IPTG will bind to the *T7* promoter and control the expression of GFP–LuxR fusion as an output signal. The LuxR produced here was again used to bind to the P_{luxI} promoter, this time as the input signal, and activate secondary expression of GFP–LuxR fusion, which in turn feeds back into the amplifier loop. In this amplifier loop, the LuxR is used as the input and positive feedback signal (Nistala et al., 2010). Such a design will allow the detection mechanism to be extremely sensitive, resulting in a significant fluorescent signal from a single receptor binding event.

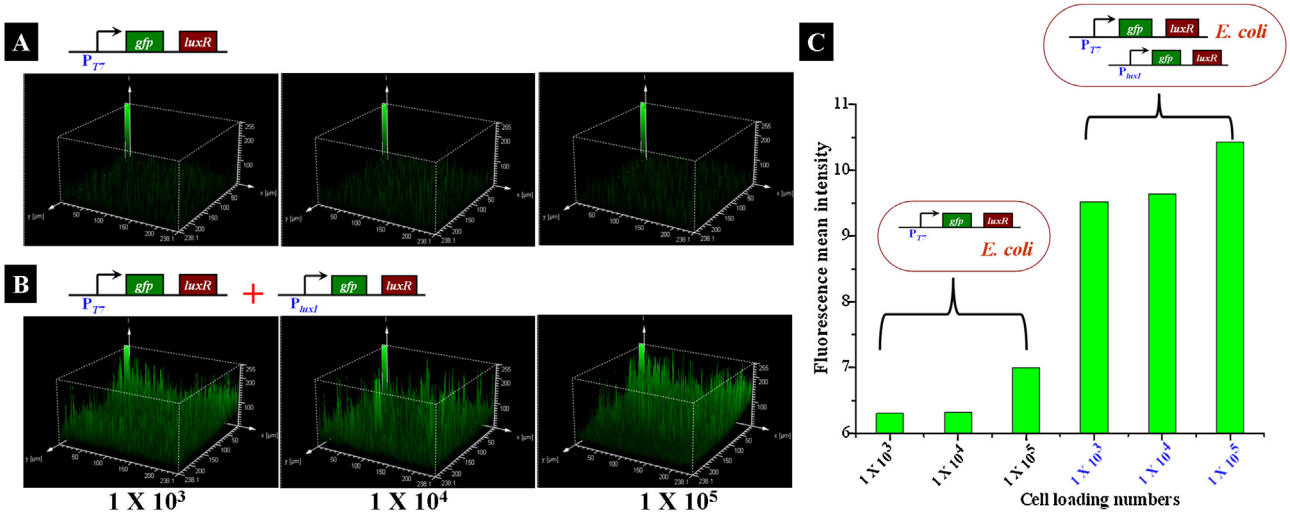

Fig. 5. Comparison of GFP signal observation in cellulose membrane without (A) and with (B) the positive-feedback genetic amplifier, as well as further comparison analysis of fluorescent intensity by ImageJ software (C).

3.5. Validation of genetic amplifier in cellulose membrane

To test the genetic amplifier designed for maximum signal, both reporter systems with and without the amplifier loop in *E. coli* strains were entrapped in cellulose membrane produced by *G. xylinus*. After cellulose membranes were produced for 4 days, different number of *E. coli* cells with and without the amplifier loop was loaded into the cellulose membranes. Fluorescent signal after IPTG induction was observed by confocal microscopy and analyzed by Image J software as described above. In the presence of the amplifier loop, IPTG will bind to the *T7* promoter and start the amplifier loop, leading to much stronger GFP fluorescent signal observed by confocal microscopy, even with a lower cell number loaded into the cellulose membranes (Fig. 5). All of the studies above confirmed that the genetic amplifier described here was able to increase the dynamic range and sensitivity of the transcriptional signal for biologically driven detection.

4. Conclusions

Extracellular cellulose pellicles produced by the bacterium *G. xylinus* can entrap itself as well as any co-cultured organisms as they grow. Our investigation demonstrated the compatibility of the cellulose-producing organism *G. xylinus* and recombinant *E. coli* strains for co-cultivation and fluorescent signal observation. The relationship between the number of entrapped *E. coli* and the level of inducible signal achieved was further examined, showing that the fluorescent signal in the cellulose membranes increased as the *E. coli* cell loading number increased. Finally a living membrane system based on a recombinant *E. coli* strain containing a positive-feedback genetic amplifier entrapped in cellulosic membranes was developed to amplify the response to inducers for maximum fluorescent signal. Such a design will allow the detection mechanism to be extremely sensitive, resulting in a significant fluorescent signal from a single receptor binding event.

Acknowledgements

We thank Prof. Kaustubh Bhalerao (University of Illinois at Urbana-Champaign, USA) for the plasmid pGN68. We would like to acknowledge the assistance of Dr. Yinan Lin for SEM studies. This work was supported by grants from the Army Research Office (58318-LS).

References

Aloni, Y., Delmer, D. P., & Benziman, M. (1982). Achievement of high rates of *in vitro* synthesis of 1,4-beta-D-glucan: Activation by cooperative interaction of the *Acetobacter xylinum* enzyme system with GTP, polyethylene glycol, and a protein factor. *Proceedings of the National Academy of Sciences of the United States of America*, *79*(21), 6448–6452.

Chao, Y., Ishida, T., Sugano, Y., & Shoda, M. (2000). Bacterial cellulose production by *Acetobacter xylinum* in a 50-L internal-loop airlift reactor. *Biotechnology and Bioengineering*, *68*(3), 345–352.

Charreau, H., Foresti, M. L., & Vazquez, A. (2012). Nanocellulose patents trends: A comprehensive review on patents on cellulose nanocrystals, microfibrillated and bacterial cellulose. *Recent Patents on Nanotechnology*.

Chepurnykh, O. E., & Avkhimenko, M. M. (1994). Ecologic and hygienic problems of elimination of chemical weapon (review). *Gigiena i Sanitariia*, (7), 36–39.

Dark, P. M., Dean, P., & Warhurst, G. (2009). Bench-to-bedside review: The promise of rapid infection diagnosis during sepsis using polymerase chain reaction-based pathogen detection. *Critical Care*, *13*(4), 217.

Gretz, M. R., Folsom, D. B., & Brown, R. M., Jr. (1989). Cellulose biogenesis in bacteria and higher plants is disrupted by magnetic fields. *Naturwissenschaften*, *76*(8), 380–383.

Henderson, L. W., & Chenoweth, D. E. (1985). Cellulose membranes – Time for a change? *Contributions to Nephrology*, *44*, 112–126.

Hwang, J. W., Yang, Y. K., Hwang, J. K., Pyun, Y. R., & Kim, Y. S. (1999). Effects of pH and dissolved oxygen on cellulose production by *Acetobacter xylinum* BRC5 in agitated culture. *Journal of Bioscience and Bioengineering*, *88*(2), 183–188.

Kim, J. S., Lee, Y. Y., & Torget, R. W. (2001). Cellulose hydrolysis under extremely low sulfuric acid and high-temperature conditions. *Applied Biochemistry and Biotechnology*, *91–93*, 331–340.

Kojima, S., Harada-Shiba, M., Nomura, S., Kimura, G., Tsushima, M., Kuramochi, M., et al. (1991). Effect of nafamostat mesilate on bradykinin generation during low-density lipoprotein apheresis using a dextran sulfate cellulose column. *ASAIO Transactions*, *37*(4), 644–648.

Lee, J. W., Deng, F., Yeomans, W. G., Allen, A. L., Gross, R. A., & Kaplan, D. L. (2001). Direct incorporation of glucosamine and N-acetylglucosamine into exopolymers by *Gluconacetobacter xylinus* (=*Acetobacter xylinum*) ATCC 10245: Production of chitosan-cellulose and chitin-cellulose exopolymers. *Applied and Environmental Microbiology*, *67*(9), 3970–3975.

Ligon, B. L. (2006). Plague: A review of its history and potential as a biological weapon. *Seminars in Pediatric Infections Diseases*, *17*(3), 161–170.

Lin, F. C., Brown, R. M., Jr., Cooper, J. B., & Delmer, D. P. (1985). Synthesis of fibrils *in vitro* by a solubilized cellulose synthase from *Acetobacter xylinum*. *Science*, *230*(4727), 822–825.

Mandal, B. B., Grinberg, A., Gil, E. S., Panilaitis, B., & Kaplan, D. L. (2012). High-strength silk protein scaffolds for bone repair. *Proceedings of the National Academy of Sciences of the United States of America*, *109*(20), 7699–7704.

Mayer, R., Ross, P., Weinhouse, H., Amikam, D., Volman, G., Ohana, P., et al. (1991). Polypeptide composition of bacterial cyclic diguanylic acid-dependent cellulose synthase and the occurrence of immunologically crossreacting proteins in higher plants. *Proceedings of the National Academy of Sciences of the United States of America*, *88*(12), 5472–5476.

Nagai, T., Nishibe, Y., Makino, Y., Tomimori, T., & Yamada, H. (1997). Enhancement of *in vivo* anti-influenza virus activity of 5,7,4′-trihydroxy-8-methoxyflavone by drug delivery system using hydroxypropyl cellulose. *Biological & Pharmaceutical Bulletin*, *20*(10), 1082–1085.

Nistala, G. J., Wu, K., Rao, C. V., & Bhalerao, K. D. (2010). A modular positive feedback-based gene amplifier. *Journal of Biological Engineering*, *4*, 4.

Park, S. H., Gil, E. S., Mandal, B. B., Cho, H., Kluge, J. A., Min, B. H., et al. (2012). Annulus fibrosus tissue engineering using lamellar silk scaffolds. *Journal of Tissue Engineering and Regenerative Medicine*.

Plumbridge, J. (1995). Co-ordinated regulation of amino sugar biosynthesis and degradation: The NagC repressor acts as both an activator and a repressor for the transcription of the glmUS operon and requires two separated NagC binding sites. *EMBO Journal*, *14*(16), 3958–3965.

Qin, G., Lapidot, S., Numata, K., Hu, X., Meirovitch, S., Dekel, M., et al. (2009). Expression, cross-linking, and characterization of recombinant chitin binding resilin. *Biomacromolecules*, *10*(12), 3227–3234.

Qin, G., Rivkin, A., Lapidot, S., Hu, X., Preis, I., Arinus, S. B., et al. (2011). Recombinant exon-encoded resilins for elastomeric biomaterials. *Biomaterials*, *32*(35), 9231–9243.

Ross, P., Mayer, R., & Benziman, M. (1991). Cellulose biosynthesis and function in bacteria. *Microbiology and Molecular Biology Reviews*, *55*(1), 35–58.

Ross, P., Weinhouse, H., Aloni, Y., Michaeli, D., Weinberger-Ohana, P., Mayer, R., et al. (1987). Regulation of cellulose synthesis in *Acetobacter xylinum* by cyclic diguanylic acid. *Nature*, *325*(6101), 279–281.

Ryu, J. H., Lee, H., Kim, Y. J., Kang, Y. S., & Kim, H. S. (2001). Facilitated olefin transport by reversible olefin coordination to silver ions in a dry cellulose acetate membrane. *Chemistry*, *7*(7), 1525–1529.

Setyawati, M. I., Chien, L. J., & Lee, C. K. (2007). Expressing Vitreoscilla hemoglobin in statically cultured *Acetobacter xylinum* with reduced O(2) tension maximizes bacterial cellulose pellicle production. *Journal of Biotechnology*, *132*(1), 38–43.

Son, H. J., Heo, M. S., Kim, Y. G., & Lee, S. J. (2001). Optimization of fermentation conditions for the production of bacterial cellulose by a newly isolated *Acetobacter* sp. A9 in shaking cultures. *Biotechnology and Applied Biochemistry*, *33*(Pt 1), 1–5.

Thomas, S. (2008). A review of the physical, biological and clinical properties of a bacterial cellulose wound dressing. *Journal of Wound Care*, *17*(8), 349–352.

Upadhyayula, V. K. (2012). Functionalized gold nanoparticle supported sensory mechanisms applied in detection of chemical and biological threat agents: A review. *Analytica Chimica Acta*, *715*, 1–18.

Yadav, V., Panilaitis, B., Shi, H., Numuta, K., Lee, K., & Kaplan, D. L. (2011). N-acetylglucosamine 6-phosphate deacetylase (nagA) is required for N-acetyl glucosamine assimilation in *Gluconacetobacter xylinus*. *PLoS ONE*, *6*(6), e18099.

Yadav, V., Paniliatis, B. J., Shi, H., Lee, K., Cebe, P., & Kaplan, D. L. (2010). Novel *in vivo*-degradable cellulose-chitin copolymer from metabolically engineered *Gluconacetobacter xylinus*. *Applied and Environmental Microbiology*, *76*(18), 6257–6265.